

A dispersive approach to the CP conserving $K \rightarrow \pi \ell^+ \ell^-$ radiative decays

Véronique Bernard^a, Sébastien Descotes-Genon^a, Marc Knecht^b, and Bachir Moussallam^a

^aUniversité Paris-Saclay, CNRS/IN2P3, IJCLab, 91405 Orsay, France

^bCNRS/Aix-Marseille Univ./Univ. de Toulon, Centre de Physique Théorique (UMR 7332), CNRS-Luminy Case 907, 13288 Marseille Cedex 9, France

March 11, 2026

Abstract

We reconsider the constraints on the form factors $W_+(s)$ and $W_S(s)$, describing the radiative decay modes $K^+ \rightarrow \pi^+ \ell^+ \ell^-$ and $K_S \rightarrow \pi^0 \ell^+ \ell^-$, associated with the general properties of analyticity and unitarity. Starting from the simple consideration of the asymptotic behaviours of the two combinations $2W_+(s) - W_S(s)$ and $W_+(s) + W_S(s)$, we derive a minimal pair of dispersive representations which involves only two free parameters. An important input for these representations consists of the $K \rightarrow 3\pi$ decay amplitudes, for which we use a set of solutions of the Khuri-Treiman equations obtained recently. These solutions provide an extrapolation from the physical $K \rightarrow 3\pi$ decay region up to the resonant $K\pi \rightarrow \pi\pi$ scattering regions. We show that the experimental energy dependence of $|W_+|^2$ can be well reproduced and that the sign of W_+ is unambiguously determined. We also show that the yet unknown $\Delta I = 1/2$ part of the $K_S \rightarrow \pi^+ \pi^- \pi^0$ amplitude can be determined from the value of $W_+(0) + W_S(0)$. The possibility of fixing the sign of $W_S(0)$ using experimental data on both $|W_+|^2$ and $|W_S|^2$ is discussed.

Contents

1	Introduction	2
2	Analyticity and unitarity	4
2.1	Local and non-local contributions	4
2.2	Unitarity: $\pi\pi$ and $K\pi$ contributions	6
2.3	Anomalous threshold	8

3	A minimal set of dispersive representations	9
3.1	Asymptotic behaviour of $W^{[1/2]}(s; \nu)$ and $W^{[3/2]}(s; \nu)$	9
3.2	Muskhelishvili-Omnès representations	9
4	Evaluation of the dispersion relations	12
4.1	Input for the $\pi\pi$ and $K\pi$ form factors	12
4.2	Input for the $K\pi \rightarrow \pi\pi$ amplitudes	14
5	Results	16
5.1	$K \rightarrow 3\pi$: Dispersive amplitudes versus their X, Y expansion	16
5.2	Determination of $\tilde{\mu}_1$	17
5.3	Results for $W_+(s)$	19
5.4	Results for $W_S(s)$	20
5.5	Additional contributions: ω and ϕ resonances	22
5.6	Additional contributions: higher mass resonances	25
6	Conclusions	26

1 Introduction

The Kaon is the next-to-lightest hadron, yet it is sensitive to physics at scales considerably larger than its mass, which allowed for instance the discovery of CP violation [1]. Of particular relevance in this regard are the CP-conserving rare radiative decay modes $K^\pm \rightarrow \pi^\pm \ell^+ \ell^-$ and $K_S \rightarrow \pi^0 \ell^+ \ell^-$. The latter amplitude is of interest because it makes an indirect CP-violating contribution to the $K_L \rightarrow \pi^0 \ell^+ \ell^-$ amplitude. This ultra-rare mode which is dominantly induced by short distance local operators, is part of the “golden modes”, together with the modes $K^\pm \rightarrow \pi^\pm \nu \bar{\nu}$, $K_L \rightarrow \pi^0 \nu \bar{\nu}$, which are able to probe the CKM dynamics of the Standard Model (SM) with a high theoretical accuracy (see e.g. ref. [2] for a summary of recent achievements in Kaon physics and future plans). A precise evaluation of this indirect CP violating contribution to the decay rate requires information on both the modulus and the phase of the K_S radiative amplitude relative to that of the direct CP violating one.

Concerning the charged amplitude $K^\pm \rightarrow \pi^\pm \ell^+ \ell^-$, several experiments have performed measurements of both the branching fraction and the decay distribution as a function of the dilepton energy s , in the e^+e^- [3, 4] as well as in the $\mu^+\mu^-$ mode [5, 6]. Comparing the e^+e^- and $\mu^+\mu^-$ amplitudes was shown to provide constraints on a class of operators which violate lepton flavour universality [7, 8]. The most recent results by the NA62 collaboration are based on a sample of 28000 events in the muon mode. The collaboration expects to collect over 100K events in each of the $\ell^+ \ell^-$ modes at the end of the present run.

In the case of the neutral mode $K_S \rightarrow \pi^0 \ell^+ \ell^-$, in contrast, only 7 events have been observed in the e^+e^- mode [9] and 6 events in the $\mu^+\mu^-$ mode [10]. New measurements are expected to

be performed by the LHCb collaboration which should be able to improve the statistics by a factor of 40 approximately [11, 12] in the $\mu^+\mu^-$ mode.

Arguments have been proposed which favour a positive sign for the interference term between the direct and indirect CP-violating contributions to the $K_L \rightarrow \pi^0\ell^+\ell^-$ amplitude [13, 14]. More recently, it has been shown [15] that a positive interference is actually a property of QCD in the limit where the number of colours N_c becomes infinite. In principle, lattice QCD is the most appropriate approach for evaluating this sign from first principles, but the present results on the radiative amplitudes are not yet sufficiently precise [16]. In this context, it would be useful to determine both the magnitude and the (appropriately defined¹) phase of the $K_S \rightarrow \pi^0\ell^+\ell^-$ amplitude from experiment, given a theoretical framework for analysing the data. The framework that has been usually employed is the so-called “beyond one-loop model” (B1L) proposed in ref. [17]. As compared with the calculation in the chiral expansion at order p^4 [18, 19] the B1L model includes terms of higher chiral order, which are needed in order to properly describe the experimental energy dependence. The B1L amplitudes are written as follows

$$W_{+,S}(s) = G_F m_K^2 \left(a_{+,S} + b_{+,S} \frac{s}{m_K^2} \right) + W_{+,S}^{\pi\pi}(s) \quad (1)$$

where the parts linear in s involve four parameters to be determined from experiment and the functions $W_{+,S}^{\pi\pi}$ account for the $\pi^+\pi^-$ channel in the unitarity relation, inducing a non linear energy dependence around the $\pi\pi$ threshold. These unitarity contributions (as we will review below) are associated with the $K^\pm \rightarrow \pi^+\pi^-\pi^\pm$ and the $K_S \rightarrow \pi^+\pi^-\pi^0$ amplitudes, respectively. In the B1L model, these are described using quadratic expansions in terms of the Dalitz parameters X, Y determined from the experimental $K \rightarrow 3\pi$ data (see the review [20]). Performing fits of the experimental data on $|W_+(s)|^2$ using the B1L model favours, in general, a negative value for a_+ (see [21]). Concerning W_S , from the available measurements of the branching fractions it is not possible to determine a_S and b_S independently without additional assumptions. The modulus of a_S has been estimated in ref. [13] assuming a vector-dominance type relation $b_S/a_S = m_K^2/m_\rho^2$ (the sign of this ratio agrees with that obtained in the large N_c calculation of ref. [15] but the magnitude differs by a factor of two).

Motivated by the continued experimental progress, and the hope to reduce the number of free parameters, we develop in this paper a dispersive description of the amplitudes W_+, W_S , i.e. based on the general non-perturbative properties of unitarity and analyticity. A similar approach has been applied previously to the radiative di-photon amplitude $K_L \rightarrow \pi^0 2\gamma$ [22]. This is performed in two steps: 1) We use the $K \rightarrow 3\pi$ amplitudes provided in ref. [23], which involve a set of 11 independent solutions of the Khuri-Treiman (KT) integral equations [24, 25]. These amplitudes have a domain of validity which extends beyond the physical decay region and can describe the scattering $K\pi \rightarrow \pi\pi$ in the region of the $\rho(770)$ resonance. 2) We include the $K\pi$ channels, in addition to $\pi^+\pi^-$, in the unitarity relation. This was not done previously,

¹We will define this phase here relative to the (non-perturbative) chiral coupling G_8 . In order to correctly compute the interference term in the $K_L \rightarrow \pi^0\ell^+\ell^-$ branching fraction knowledge of the relative phase between G_8 and the imaginary part of the perturbative parameter C_{7V} is also necessary.

but it proves important, from a formal point of view, in order to obtain a representation which achieves a consistent cancellation of the QCD scale dependence upon adding the long-distance contribution and the short-distance one from the local operator Q_{7V} at any value of the energy s . Considering the asymptotic behaviour we will show that a pair of dispersive representations which involves only two parameters (which can be taken as a_+ , a_S) should hold. Finally, as an effect of $K^+\pi^- \rightarrow K^0\pi^0$ scattering, our representation couples the two amplitudes W_+ , W_S such that, in principle, information on both a_+ and a_S can be extracted from data on a single amplitude e.g. W_+ .

The plan of the paper is as follows. We first introduce in sec. 2 the notation and the various definitions and write the unitarity relations associated with the $\pi\pi$ and the $K\pi$ two-body channels. In order to deal with $K\pi$ we introduce two combinations of the amplitudes W_+ , W_S which correspond to the $K\pi$ isospins $I = 1/2$ and $I = 3/2$. The $\pi\pi$ contribution is affected by the presence of an anomalous threshold which is discussed in sec. 2.3. Before writing the dispersive representations, we examine the asymptotic behaviour which is found to depend on the $K\pi$ isospin. The dispersive representations, which are of the Muskhelishvili-Omnès type [26, 27], are then written down in eqs. (21) and (24). Then, in sec. 4, the various inputs which are needed in the evaluation of the dispersive representations, i.e. the $\pi\pi$ and $K\pi$ form factors as well as the $K \rightarrow 3\pi$ amplitudes are discussed. These are known, except for the $\Delta I = 1/2$ component of the $K_S \rightarrow \pi^+\pi^-\pi^0$ amplitude which has not yet been determined from the decay data, because it is chirally suppressed, but plays a role in the dispersive integrals. We will show that, given the values of the two parameters a_+ and a_S , one can determine both this component of the $K_S \rightarrow \pi^+\pi^-\pi^0$ amplitude and the W_+ , W_S form factors. The results, finally, are presented in sec. 5.

2 Analyticity and unitarity

2.1 Local and non-local contributions

The radiative decays $K^+ \rightarrow \pi^+\ell^+\ell^-$ and $K_S \rightarrow \pi^0\ell^+\ell^-$ ($\ell = e, \mu$) are flavour-changing neutral-current (FCNC) processes that are suppressed in the standard model. They are induced by γ -penguin, Z -penguin and W -box diagrams [28, 29, 30]. At low energies (below the charm mass), these diagrams are represented by local operators involving only the three light quarks u, d, s . They consist of a set of four-quark operators (we use the notation of ref. [31])

$$\mathcal{L}_{\Delta S=1}(x) = -\frac{G_F}{\sqrt{2}}V_{ud}V_{us}^* \sum_1^6 C_i O_i(x) \quad (2)$$

and of two operators involving the direct coupling of a leptonic vector or axial current to the neutral strangeness-changing $V - A$ current,

$$\mathcal{L}_{\Delta S=1}^{\text{lept}}(x) = -\frac{G_F}{\sqrt{2}}V_{ud}V_{us}^* [C_{7V}(\nu)O_{7V}(x) + C_{7A}O_{7A}(x)] , \quad (3)$$

with

$$O_{7V} = \bar{s}\gamma_\mu(1 - \gamma_5)d\bar{\ell}\gamma^\mu\ell, \quad O_{7A} = \bar{s}\gamma_\mu(1 - \gamma_5)d\bar{\ell}\gamma^\mu\gamma^5\ell. \quad (4)$$

In the sequel we will neglect all CP-violating effects. This means that the imaginary parts of the Wilson coefficients C_i and C_{7V} , C_{7A} are discarded and that K_S will be identified with the CP-even combination of K^0 and \bar{K}^0 . Moreover, we will not consider the contribution from $O_{7A}(x)$ since it plays no role in our analysis and since its contribution to the amplitude is tiny anyway. The contributions to the radiative amplitudes associated with the local operator O_{7V} can be written in terms of the semi-leptonic $K\pi$ form factors $f_+^{K\pi}$, $f_-^{K\pi}$ assuming isospin symmetry,

$$\langle \pi^+(p_2) | \bar{s}\gamma_\mu d | K^+(p_1) \rangle = -\langle \pi^0(p_2) | \bar{s}\gamma_\mu d | K_S(p_1) \rangle = (p_1 + p_2)_\mu f_+^{K\pi}(s) + (p_1 - p_2)_\mu f_-^{K\pi}(s). \quad (5)$$

The radiative amplitudes receive additional non-local contributions involving a virtual photon, which are associated with the matrix elements

$$\langle \pi | T \{ j_\mu^{em}(0) i\mathcal{L}_{\Delta S=1}(x) \} | K \rangle \quad (6)$$

where $j_\mu^{em} = \frac{2}{3}\bar{u}\gamma_\mu u - \frac{1}{3}(\bar{d}\gamma_\mu d + \bar{s}\gamma_\mu s)$ is the electromagnetic current of three-flavour QCD. Using the same notation as in ref. [21] the two $K \rightarrow \pi\gamma^*$ form factors are defined as follows

$$\begin{aligned} \int d^4x \langle \pi^+(p_2) | T \{ j_\mu^{em}(0) i\mathcal{L}_{\Delta S=1}(x) \} | K^+(p_1) \rangle &= \frac{2W_+(s; \nu)}{16\pi^2 m_K^2} Q_\mu, \\ \int d^4x \langle \pi^0(p_2) | T \{ j_\mu^{em}(0) i\mathcal{L}_{\Delta S=1}(x) \} | K^0(p_1) \rangle &= \frac{\sqrt{2}W_S(s; \nu)}{16\pi^2 m_K^2} Q_\mu, \end{aligned} \quad (7)$$

with

$$Q_\mu = \frac{s}{2}(p_1 + p_2)_\mu - \frac{\Delta_{K\pi}}{2}(p_1 - p_2)_\mu, \quad (8)$$

where $s = (p_1 - p_2)^2$ is the photon virtuality and $\Delta_{K\pi} = m_K^2 - m_\pi^2$. This non-local part of the form factors depends on a renormalisation scale ν [30, 21], which reflects the fact that the time-ordered product in eq. (6) is singular at short distances [32] and needs to be regularised.

Physical form factors (which do not depend on the renormalisation scale) are obtained by adding the non-local and local contributions

$$\begin{aligned} W_+(s) &= W_+(s; \nu) + 4\pi \frac{G_F m_K^2 V_{ud} V_{us}^*}{\sqrt{2} \alpha} C_{7V}(\nu) f_+^{K\pi}(s), \\ W_S(s) &= W_S(s; \nu) - 4\pi \frac{G_F m_K^2 V_{ud} V_{us}^*}{\sqrt{2} \alpha} C_{7V}(\nu) f_+^{K\pi}(s). \end{aligned} \quad (9)$$

We will construct dispersive representations of the form factors $W_{+,S}(s)$ assuming that they satisfy the usual analyticity properties.

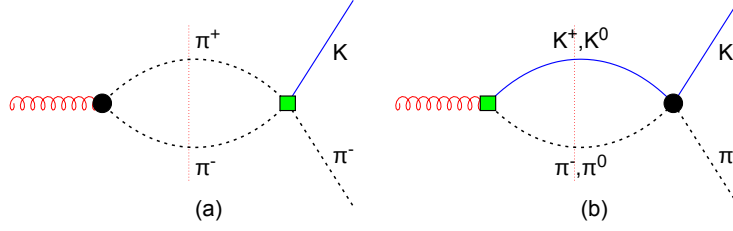


Figure 1: Contributions to the unitarity relation from the $\pi\pi$ and the $K\pi$ states. A black dot represents an electromagnetic or strong vertex, a green square denotes a weak $\Delta S = 1$ vertex

2.2 Unitarity: $\pi\pi$ and $K\pi$ contributions

We discuss here the contributions from the $\pi\pi$ and $K\pi$ states in the unitarity relations (see fig. 1) of the form factors $W_{+,S}$, which we will be able to evaluate in a model independent way based on experimental input. The two-pion state is the lightest hadronic state that contributes to the discontinuities of the form factors. In the low-energy chiral expansion this contribution starts at order p^4 and is the dominant one [18]. It is also important from a dispersive point of view because it displays a resonance peak associated with the $\rho(770)$ meson. The discontinuities² associated with $\pi^+\pi^-$, illustrated in fig. 1(a), take the form

$$\begin{aligned} \frac{\text{disc}[W_+(s)]_{\pi\pi}}{16\pi^2 m_K^2} &= \frac{\theta(s - 4m_\pi^2)}{16\pi} \left(1 - \frac{4m_\pi^2}{s}\right)^{3/2} [F_V^{\pi\pi}(s)]^* \times f_1^{K^+\pi^- \rightarrow \pi^+\pi^-}(s), \\ \frac{\text{disc}[W_S(s)]_{\pi\pi}}{16\pi^2 m_K^2} &= \frac{\theta(s - 4m_\pi^2)}{16\pi} \left(1 - \frac{4m_\pi^2}{s}\right)^{3/2} [F_V^{\pi\pi}(s)]^* \times f_1^{K_S\pi^0 \rightarrow \pi^+\pi^-}(s), \end{aligned} \quad (10)$$

where $F_V^{\pi\pi}(s)$ is the electromagnetic form factor of the pion,

$$\langle \pi^+(p_2) | j_\mu^{em}(0) | \pi^+(p_1) \rangle = (p_1 + p_2)_\mu F_V^{\pi\pi}((p_1 - p_2)^2), \quad (11)$$

and $f_1^{K\pi \rightarrow \pi\pi}$ is the $J = 1$ partial-wave projection of the $K\pi \rightarrow \pi\pi$ amplitude,

$$f_1^{K\pi \rightarrow \pi\pi}(s) = \frac{1}{2\kappa(s)} \int_{-1}^1 dz z \mathcal{A}_{K\pi \rightarrow \pi\pi}(s, t(z), u(z)), \quad (12)$$

with $\kappa(s) = \sqrt{(s - m_-^2)(s - m_+^2)(1 - 4m_\pi^2/s)}$, $m_\pm = m_K \pm m_\pi$. The Mandelstam variables s , t , u in the $K(p_K)\pi(p_3) \rightarrow \pi(p_1)\pi(p_2)$ amplitudes being defined as

$$s = (p_K + p_3)^2, \quad t = (p_K - p_1)^2, \quad u = (p_K - p_2)^2, \quad s + t + u = 3s_0, \quad s_0 \equiv \frac{m_K^2}{3} + m_\pi^2 \quad (13)$$

²The discontinuity is defined as $\text{disc}[W(s)] \equiv (W(s + i\epsilon) - W(s - i\epsilon))/(2i)$.

the dependence of the variables t, u on the scattering angle θ in the $\pi^+\pi^-$ centre-of-mass system is given by

$$t(z), u(z) = \frac{1}{2} (3s_0 - s \pm \kappa(s) z) , \quad z = \cos \theta. \quad (14)$$

Next, the contributions from the $K^+\pi^-$ and $K^0\pi^0$ states to the unitarity relation are illustrated in fig 1(b). As can be seen from the figure, they are proportional to the form factors themselves and to $K\pi \rightarrow K\pi$ amplitudes. Since $K^0\pi^0$ can scatter to $K^+\pi^-$ and vice versa these unitarity contributions induce a coupling between W_+ and W_S . It is convenient, then, to express the dispersion relations in terms of the form factors which correspond to the $K\pi$ isospins $I = 1/2$ and $I = 3/2$ combinations that diagonalise the S -matrix in the $K\pi \rightarrow K\pi$ subspace, assuming isospin conservation

$$\begin{aligned} W^{[1/2]}(s) &\equiv 2W_+(s) - W_S(s) \\ W^{[3/2]}(s) &\equiv W_+(s) + W_S(s) . \end{aligned} \quad (15)$$

In the energy region where $K\pi \rightarrow K\pi$ scattering is elastic the $K\pi$ unitarity relations can be simply expressed as follows in terms of the $J = 1$ elastic $K\pi$ phase-shifts δ_1^I

$$\begin{aligned} \text{disc} [W^{[1/2]}(s)]_{K\pi, \text{elastic}} &= \exp(-i\delta_1^{1/2}(s)) \sin(\delta_1^{1/2}(s)) W^{[1/2]}(s) \\ \text{disc} [W^{[3/2]}(s)]_{K\pi, \text{elastic}} &= \exp(-i\delta_1^{3/2}(s)) \sin(\delta_1^{3/2}(s)) W^{[3/2]}(s) . \end{aligned} \quad (16)$$

In the chiral expansion, these $K\pi$ contributions start at order p^6 but they are important in a dispersive framework, at least in the $I = 1/2$ channel, where they are associated to the peak of the $K^*(892)$ resonance. Furthermore, we stress that the contribution from the local operators (5) naturally drops out of the combination $W^{[3/2]}(s)$, and that the discontinuity equation (16) for $W^{[1/2]}(s)$ holds for each component, local and non-local, separately, and hence for the scale-independent sum.

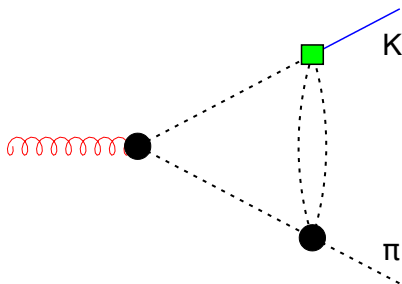


Figure 2: Graph giving rise to an anomalous threshold

2.3 Anomalous threshold

It has been noticed long ago that triangle-type Feynman diagrams can exhibit anomalous thresholds [33]. In some situations, these lead to cuts and the associated contributions must be added to the one from the unitarity cut. A recent detailed discussion can be found in ref. [34]. In the case of the form factors $W_{+,S}(s)$ considered here, using the formulas from ref. [33] one finds that an anomalous threshold is indeed present, associated with the diagram shown in fig. 2. It is located at the point $s_{\text{anom}} = (m_K - m_\pi)^2$ belonging to the real axis above the $\pi\pi$ threshold. In this situation, no additional cut contribution is required (the situation is quite different in the case of, e.g., the $B \rightarrow K\gamma^*$ form factors discussed in [34]). The anomalous threshold is associated with a singularity of the form $(s_{\text{anom}} - s)^{-3/2}$ induced in the discontinuity functions $\text{disc}[W_{+,S}(s)]_{\pi\pi}$ by the $J = 1$ partial-wave amplitude $f_1^{K\pi \rightarrow \pi\pi}(s)$ (see fig. 8). This singularity appears at the turning point of the complex left-hand cut of this amplitude which is illustrated in fig. 3. This complex cut partly overlaps with the unitarity $\pi\pi$ cut but it can be displaced from the real axis by performing an infinitesimal imaginary shift of the kaon mass: $m_K^2 \rightarrow m_K^2 + i\epsilon$ (e.g. [35] for a review in the case of $\eta \rightarrow 3\pi$) such that the integral along the unitarity cut is well defined.

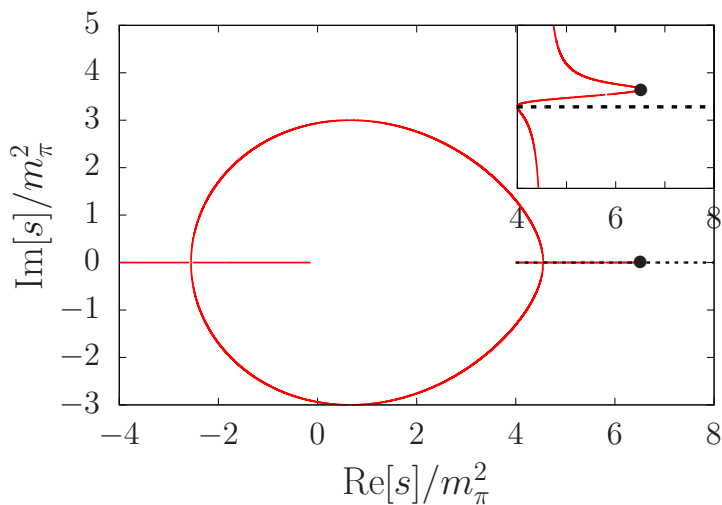


Figure 3: Complex left-hand cut of the $K\pi \rightarrow \pi\pi$ partial-wave amplitudes (red line). The dotted line represents the unitarity cut. The sub-figure shows an enlarged view of the vicinity of the positive real axis illustrating the effect of performing an infinitesimal imaginary shift of m_K which separates the complex cut from the unitarity cut. The black dot shows the position of the singularity.

3 A minimal set of dispersive representations

3.1 Asymptotic behaviour of $W^{[1/2]}(s; \nu)$ and $W^{[3/2]}(s; \nu)$

The behaviour of the form factors $W_{+,s}(s; \nu)$ for large space-like values of s can be deduced from the operator-product expansion of the time-ordered product (6) that drives the $K \rightarrow \pi\gamma^*$ transitions. The leading term in this expansion is a dimension 3 operator (see refs. [21] and [36] for a detailed discussion) and the corresponding leading large-momentum behaviour has the following form

$$\lim_{q \rightarrow \infty} \int d^4x e^{iq \cdot x} T \{ j_\mu^{em}(x) \mathcal{L}_{\Delta S=1}(0) \} = (q_\mu q_\nu - g_{\mu\nu} q^2) (A + B \ln \frac{-q^2}{\nu^2} + \dots) [\bar{s} \gamma_\nu (1 - \gamma^5) d] \quad (17)$$

where the ellipsis stands for $O(\alpha_s)$ corrections. The operator $[\bar{s} \gamma_\nu (1 - \gamma^5) d]$ which appears in this expression carries isospin $I = 1/2$. It thus contributes only to the matrix element $W^{[1/2]}$ and not to $W^{[3/2]}$, in agreement with the absence, already noticed earlier, of a ν -dependent contribution to $W^{[3/2]}$ from the local operator O_{7V} . One can verify, at lowest order, that the scale dependence in eq. (17) is exactly the one needed to cancel the dependence from $C_{7V}(\nu)$ [21] in the total form factors (9). Taking the $K\pi$ matrix element of eq. (17) one deduces that the ratio $W^{[1/2]}(s; \nu)/f_+^{K\pi}(s)$ behaves as $\sim \log(s)$ asymptotically and thus satisfies a convergent dispersive representation with one subtraction.

The behaviour of $W^{[3/2]}(s; \nu)$ at large space-like values of s is controlled by subleading operators in the short-distance expansion: one needs to go up to dimension-6 four-quark operators in order to find one with an isospin $I = 3/2$ component, e.g.

$$\int d^4x e^{iq \cdot x} T \{ j^\mu(x) \mathcal{L}_{\Delta S=1}^{eff}(0) \}_{\dim=6} \sim \left[C_V^{(6)}(\nu) \frac{g^{\mu\beta} q^\alpha - g^{\mu\alpha} q^\beta}{q^2} + C_A^{(6)}(\nu) \epsilon^{\mu\nu\alpha\beta} \frac{q_\nu}{q^2} \right] \times (\bar{s} \gamma_\alpha u) (\bar{u} \gamma_\beta d) . \quad (18)$$

As a consequence of this smooth behaviour at short distances, we can make the plausible assumption that the combination $W^{[3/2]}(s)$ satisfies a dispersive representation without any subtraction.

3.2 Muskhelishvili-Omnès representations

The discontinuities of the form factors across the $K\pi$ cut inside the elastic scattering region, given in eqs. (16), have the form which leads to integral equations of the Muskhelishvili-Omnès type [26, 27]. These equations are solved in terms of the Omnès functions $\Omega_1^{1/2}(s)$ and $\Omega_1^{3/2}(s)$,

$$\Omega_1^I(s) = \exp \left[\frac{s}{\pi} \int_{m_+^2}^{\infty} ds' \frac{\delta_1^I(s')}{s'(s' - s)} \right] \quad (19)$$

where $m_+ = m_\pi + m_K$. The $K\pi$ phases $\delta_1^I(s)$ to be used in these integrals must be equal to the elastic scattering phase-shifts in the elastic region and can be chosen in a somewhat arbitrary way above that region. It is noteworthy that the elastic region extends effectively well above the first inelastic threshold $K\pi\pi$, up to $\Lambda = 1.3$ GeV approximately [37]. The $J = 1, I = 3/2$ phase-shift is very small and will be simply interpolated to zero above 1 GeV. In the case of $I = 1/2$ we can use the $K\pi$ vector form factor (the modulus of which is a measurable quantity) i.e. take $\Omega_1^{1/2}(s) \equiv f_+^{K\pi}(s)/f_+^{K\pi}(0)$ which obeys eq. (19) with a phase given by the $K\pi$ form factor phase in the inelastic region.

We first consider the $I = 3/2$ combination $W^{[3/2]}(s)$ and define the following cut-analytic function

$$\Phi^{[3/2]}(s) = \frac{W^{[3/2]}(s)}{\Omega_1^{[3/2]}(s)}. \quad (20)$$

Then, the discontinuity across the $K\pi$ cut of the Omnès function in the denominator cancels exactly the discontinuity of $W^{[3/2]}(s)$ in the numerator, such that the function $\Phi^{[3/2]}(s)$ no longer has a $K\pi$ cut (below $\Lambda \approx 1.3$ GeV). The function $\Phi^{[3/2]}(s)$ is left with the cut associated with $\pi\pi$ firstly, but also with unitarity cuts associated with higher-mass states like $3\pi, K\bar{K}, \dots$. One remarks, however, that the contributions from the $I = 0$ resonances $\omega(782), \phi(1020)$ associated with these discontinuities should be strongly reduced by the $\Delta I = 1/2$ rule as compared to the contribution from the $I = 1$ resonance $\rho(770)$ to $\pi\pi$. It thus seems a good approximation to retain only the contribution from the $\pi\pi$ cut. This leads to the following very simple representation,

$$W^{[3/2]}(s) = \Omega_1^{3/2}(s) \times \frac{1}{\pi} \int_{4m_\pi^2}^{\Lambda^2} ds' \frac{\text{disc} [W_+(s') + W_S(s')]_{\pi\pi}}{(s' - s)\Omega_1^{3/2}(s')}, \quad (21)$$

assuming also that the contributions from the inelastic region $s' > \Lambda^2$ can be neglected. The $\pi\pi$ discontinuities needed in eq. (21) were given in eq. (10).

Considering the $I = 1/2$ combination $W^{[1/2]}(s)$, in order to optimise the description of the contributing $\rho(770)$ and $K^*(892)$ resonances, we start by introducing the following once-subtracted dispersive integral over the $\pi\pi$ discontinuity

$$W_{\pi\pi}^{[1/2]}(s) \equiv \frac{s}{\pi} \int_{4m_\pi^2}^{\Lambda^2} ds' \frac{\text{disc} [2W_+(s') - W_S(s')]_{\pi\pi}}{s'(s' - s)} \quad (22)$$

(which carries the information on the $\rho(770)$) and define the following cut-analytic function

$$\Phi^{[1/2]}(s; \nu) = \frac{W^{[1/2]}(s; \nu) - W_{\pi\pi}^{[1/2]}(s)}{f_+^{K\pi}(s)}. \quad (23)$$

The function in the numerator no longer has a $\pi\pi$ cut (in the region $s < \Lambda^2$) so that $\Phi^{[1/2]}$ can be expressed in terms of the $K\pi$ discontinuity (further contributions from $3\pi, K\bar{K}...$ will be

estimated approximately below). Using one subtraction constant in the dispersive representation³ of $\Phi^{[1/2]}(s; \nu)$ and the property that the ratio $W_+^{[1/2]}/f_+^{K\pi}$ has no $K\pi$ discontinuity in the elastic region, the amplitude $W^{[1/2]}(s; \nu)$ gets expressed as follows

$$W^{[1/2]}(s; \nu) = W_{\pi\pi}^{[1/2]}(s) + f_+^{K\pi}(s) \left[C^{[1/2]}(\nu) - \frac{s}{\pi} \int_{m_+^2}^{\Lambda^2} ds' \frac{W_{\pi\pi}^{[1/2]}(s') \text{Im} [1/f_+^{K\pi}(s')]}{s'(s' - s)} \right]. \quad (24)$$

In this representation, the dependence on the scale ν must be entirely carried by the subtraction constant $C^{[1/2]}(\nu)$ since all the other terms on the right-hand side of eq. (24) are manifestly scale independent. The structure of the representation (24) is the appropriate one to allow for an exact cancellation of the ν dependence upon adding the contribution proportional to $C_{7V}(\nu)$ in eq. (9). The physical amplitude, after adding this part, can be written as

$$W^{[1/2]}(s) = W_{\pi\pi}^{[1/2]}(s) + f_+^{K\pi}(s) \left[G_F m_K^2 \frac{2a_+ - a_S}{f_+^{K\pi}(0)} - \frac{s}{\pi} \int_{m_+^2}^{\Lambda^2} ds' \frac{W_{\pi\pi}^{[1/2]}(s') \text{Im} [1/f_+^{K\pi}(s')]}{s'(s' - s)} \right] \quad (25)$$

where a_+ , a_S are proportional to the values at $s = 0$

$$W_{+,S}(0) = G_F m_K^2 a_{+,S} \quad (26)$$

following the notation of the B1L model.

At this point eqs. (21) and (25) form a system of coupled equations for the form factors $W_+(s)$ and $W_S(s)$ which exhibits an explicit dependence on a single free parameter, $2a_+ - a_S$. In order to make use of these equations, we next need to address the $K\pi \rightarrow \pi\pi$ partial-wave projections appearing in eq. (10). While our knowledge of the $K \rightarrow 3\pi$ amplitudes is rather detailed, it is, however, not fully complete. The $\Delta I = 1/2$ part of the $K_S \rightarrow \pi^+\pi^-\pi^0$ amplitude, which corresponds to the 3π state with a total isospin $I_{3\pi} = 0$ is chirally suppressed [38] and has not yet been determined from the available experimental data on the Dalitz plot distribution. In the Khuri-Treiman approach of ref. [23] this part is proportional to a parameter called $\tilde{\mu}_1$, see eqs. (32) and (35) below. The equations (21) and (25) can then be used in the following way: given the values of $W_{+,S}$ at $s = 0$, i.e. a_+ and a_S , one can first determine $\tilde{\mu}_1$ from eq. (21) that provides a linear relation between $a_+ + a_S$ and $\tilde{\mu}_1$ (see eq. (37) below). Then, the two form factors can be completely predicted for $s \neq 0$ using the two dispersive equations. We next describe how we proceed with their evaluation.

³The ratio $W^{[1/2]}(s; \nu)/f_+^{K\pi}(s)$ behaving as $\sim \log(s)$ asymptotically, as mentioned, the function $\Phi^{[1/2]}(s; \nu)$ satisfies a once-subtracted dispersion relation provided that $W_{\pi\pi}^{[1/2]}(s) \sim 1/s$ when $s \rightarrow \infty$. We assume this to be realised through a regularisation function which modifies $W_{\pi\pi}^{[1/2]}(s)$ as defined in (22) when $s \gg \Lambda^2$.

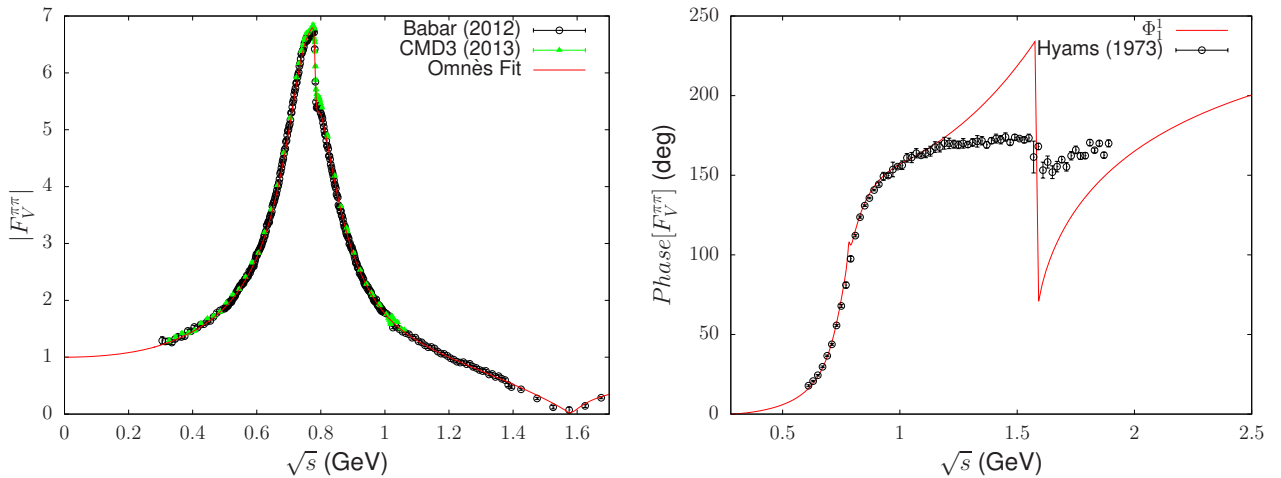


Figure 4: The phase of the $\pi\pi$ form factor used in the Omnès-type representation (right) and the resulting modulus (left).

4 Evaluation of the dispersion relations

4.1 Input for the $\pi\pi$ and $K\pi$ form factors

We describe both the $\pi\pi$ and the $K\pi$ form factors using dispersive representations analogous to (19), which properly encode both the analyticity properties and the relation between the phase and the elastic scattering phase-shift at low energy, see e.g. refs. [39, 40]. We also assume the absence of complex zeros [40] (see [41] for a recent discussion). The phase of the pion form factor, $\phi_1^1(s)$, is described in the elastic region (which we take to be $s \leq 1.44 \text{ GeV}^2$) as a sum: $\phi_1^1(s) = \delta_1^1(s) + \delta_\omega(s)$ where δ_1^1 is the $\pi\pi$ elastic scattering phase, for which we use the experimental results [42] with the same parameterisation as used in the $K \rightarrow 3\pi$ KT equations, and $\delta_\omega(s)$ is the isospin breaking contribution induced by the $\omega(782)$ resonance which we parameterise as

$$\delta_\omega(s) = \theta(s - 9m_\pi^2) \text{Arg} \left(1 + \epsilon_\omega e^{i\phi_\omega} \frac{m_\omega^2}{(m_\omega - i\Gamma_\omega/2)^2 - s} \right). \quad (27)$$

In the inelastic region we satisfy ourselves with a rough description (see ref. [43] for a recent detailed determination of this phase), since we need the form factor only in the elastic region. The free parameters in the phase are fitted to experimental data on the modulus of the form factor. Because of the importance of $F_V^{\pi\pi}$ in the evaluation of the $g - 2$ of the muon, there has been a number of measurements of this quantity in recent years using $e^+e^- \rightarrow \pi^+\pi^-$ scattering as well as $\tau^\mp \rightarrow \pi^\mp \pi^0 \nu$ decays, see the review [44]. More specifically, we have used the data from Babar [45] in the present work. The results of our fit for the modulus and the phase of $F_V^{\pi\pi}$ are shown in fig. 4.

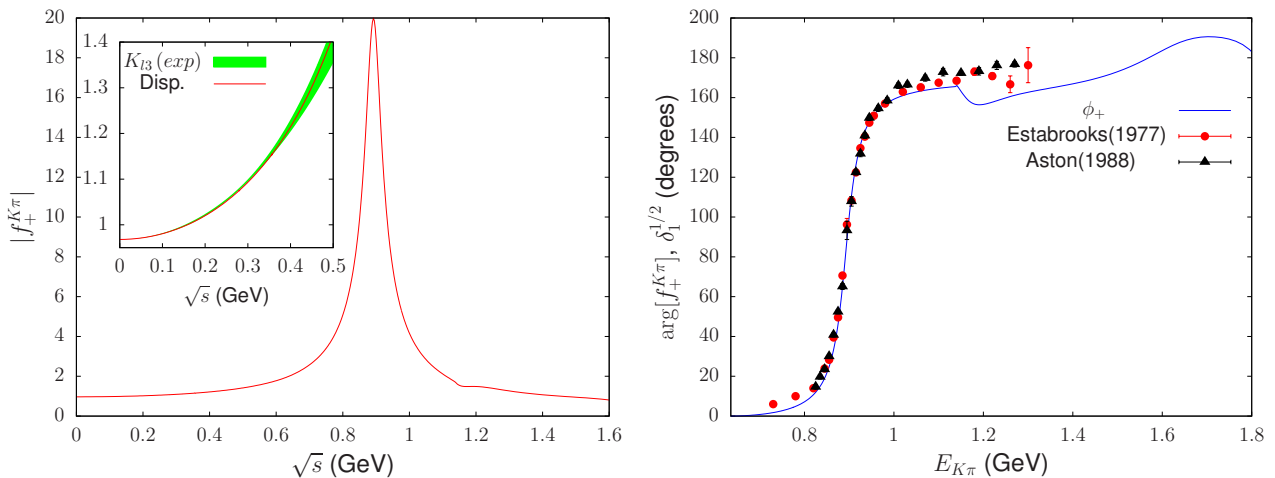


Figure 5: Phase (right) and corresponding modulus (left) of the $K\pi$ vector form factor $f_+^{K\pi}(s)$. The phase is compared with the $K\pi$ P -wave scattering phase-shift from refs. [37, 46]. The modulus is compared at low energy to a quadratic representation of experimental K_{l3} decay data[47].

The $K\pi$ vector form factor can be determined, in principle, from $\tau \rightarrow K\pi\nu$ decays and, at low energy, from K_{l3} decays. The corresponding amplitudes involve both $f_+^{K\pi}$ and the scalar form factor $f_0^{K\pi}$,

$$f_0^{K\pi}(s) \equiv f_+^{K\pi}(s) + \frac{s}{\Delta_{K\pi}} f_-^{K\pi}(s). \quad (28)$$

Several theoretical models of these two form factors have been proposed (e.g. [48, 49, 50, 51, 52]) while measurements of $\tau \rightarrow K\pi\nu$ decays have been performed by Aleph [53], Belle [54] and Babar [55]. We use here a two-channel unitary model for the scalar form factor as originally proposed in [56]. For the vector form factor we use a dispersive phase representation with a normalising value at $s = 0$, $f_+^{K\pi}(0) = 0.968$, and in which the phase $\phi_+(s)$ is constructed as follows: a) in the elastic scattering region ($\sqrt{s} \leq 1.14$ GeV) it is described as a simple Breit-Wigner function with two parameters M_{K^*} , Γ_{K^*}

$$\phi_+(s) = \arctan\left(\frac{\sqrt{s}\Gamma_{K^*}(s)}{M_{K^*}^2 - s}\right), \quad \Gamma_{K^*}(s) = \Gamma_{K^*} \frac{M_{K^*}^2}{s} \left(\frac{p_{cm}(s, m_\pi, m_K)}{p_{cm}(M_{K^*}^2, m_\pi, m_K)}\right)^{3/2} \quad (29)$$

(p_{cm} being the centre-of-mass momentum) and b) in the inelastic region the phase $\phi_+(s)$ is taken from the three-channel unitary model proposed in ref. [49]. While model dependent, this phase has the nice property of going to π asymptotically from above, as required by QCD [40], and its energy dependence reflects the presence of the $K^*(1410)$ and $K^*(1680)$ resonances. A rather good fit of the $\tau \rightarrow K\pi\nu_\tau$ Belle data [54] can be obtained in this manner with

$$M_{K^*} = (895.51 \pm 0.16) \text{ MeV}, \quad \Gamma_{K^*} = (48.25 \pm 0.35) \text{ MeV} \quad (30)$$

and a χ^2 value $\chi^2/N_{dof} = 132/98$. Fig. 5 (right) shows the phase ϕ_+ and illustrates its compatibility with the elastic P -wave scattering phase-shifts from refs. [37, 46] in the elastic energy region. The left plot shows the modulus $|f_+^{K\pi}(s)|$ computed from the dispersive phase representation. At low energy it is seen to be in very good agreement with the experimental determination from K_{l3} decays as given in ref. [47].

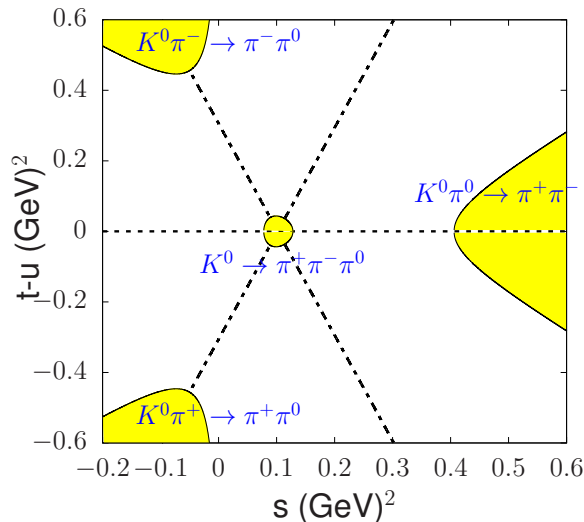


Figure 6: Illustration of the various physical regions for $K^0 \rightarrow 3\pi$ and $K^0\pi \rightarrow \pi\pi$ as a function of the Mandelstam variables s and $t - u$. Also shown are the three lines $t = u$, $s = t$, $u = s$.

4.2 Input for the $K\pi \rightarrow \pi\pi$ amplitudes

In order to compute the discontinuities displayed in eq. (10) we need the amplitudes $K\pi \rightarrow \pi\pi$ in an energy range extending from the $\pi\pi$ threshold up to physical scattering region in order to capture the effects of the $\rho(770)$ resonance. For this purpose, we rely on a set of solutions of the Khuri-Treiman equations [24, 25] recently obtained in ref. [23]. These equations, by construction, encode the properties of analyticity and elastic unitarity (for the $J = 0, 1$ partial-waves) that allow one to perform the extrapolation from the Dalitz plot region, in which $K \rightarrow 3\pi$ decay measurements can be performed, up to the physical scattering region. These various regions of the Mandelstam plane are illustrated in fig. 6.

In the KT formalism as used in [23], the $K\pi \rightarrow \pi\pi$ amplitudes are expressed in terms of a set of nine functions of one variable. Four of these ($M_0, M_1, M_2, \widetilde{M}_1$) describe $\Delta I = 1/2$ transitions and the remaining five ($N_0, N_1, N_2, \widetilde{N}_1, \widetilde{N}_2$) describe $\Delta I = 3/2$ transitions. We reproduce below the expressions of the two amplitudes which are of interest here in terms of

these functions

$$\begin{aligned} \mathcal{A}_{K^+\pi^-\rightarrow\pi^+\pi^-}(s, t, u) = & \left\{ (t-u) \left(M_1(s) + N_1(s) + \frac{3}{2}\tilde{N}_1(s) \right) \right. \\ & + M_0(t) + N_0(t) + \frac{1}{3}(M_2(t) + N_2(t)) - \frac{1}{2}\tilde{N}_2(t) \\ & \left. + (t \leftrightarrow s) \right\} + 2(M_2(u) + N_2(u)) + \tilde{N}_2(u) \end{aligned} \quad (31)$$

and

$$\begin{aligned} \mathcal{A}_{K_S\pi^0\rightarrow\pi^+\pi^-}(s, t, u) = & (t-u)\widetilde{M}_1(s) + (s-t)\widetilde{M}_1(u) + (u-s)\widetilde{M}_1(t) \\ & - 2(t-u)\tilde{N}_1(s) + \left\{ \tilde{N}_2(t) + (s-t)\tilde{N}_1(u) - (t \leftrightarrow u) \right\}. \end{aligned} \quad (32)$$

Performing the angular integrations of these amplitudes according to eq. (12) one obtains the two $J = 1$ partial waves in the following form,

$$\begin{aligned} f_1^{K^+\pi^-\rightarrow\pi^+\pi^-}(s) &= \frac{1}{3} \left(M_1(s) + N_1(s) + \frac{3}{2}\tilde{N}_1(s) + \widehat{M}_1(s) + \widehat{N}_1(s) + \frac{3}{2}\widehat{\tilde{N}}_1(s) \right) \\ f_1^{K_S\pi^0\rightarrow\pi^+\pi^-}(s) &= \frac{1}{3} \left(\widetilde{M}_1(s) + \widehat{\widetilde{M}}_1(s) - \frac{2}{3}(\tilde{N}_1(s) + \widehat{\tilde{N}}_1(s)) \right). \end{aligned} \quad (33)$$

The hat-functions, $\widehat{M}_1, \widehat{N}_1, \dots$ (following the notation introduced in [57]) in eq. (33) represent linear combinations of angular integrals of the one-variable functions (explicit expressions can be found in ref. [23]). The KT equations ensure that the partial waves $f_1^{K\pi\rightarrow\pi\pi}$ from eqs (33) satisfy the elastic $\pi\pi$ unitarity relations. They should thus be valid at low energy and up to the $\rho(770)$ mass region, but no longer at higher energy in particular in the $K^*(892)$ mass region since $K\pi$ unitarity is not implemented.

The nine one-variable functions can be expressed linearly in terms of a set of independent solutions of the Khuri-Treiman integral equations. These linear representations involve 11 subtraction constants $\mu_k, \nu_k, k = 0, 1, 2, 3, \tilde{\nu}_0, \tilde{\nu}_1$, and $\tilde{\mu}_1$. For instance, for M_1, N_1, \tilde{N}_1 one has

$$M_1(s) = \sum_{k=0}^3 \mu_k \mathcal{S}_1^{(k)}(s), \quad N_1(s) = \sum_{k=0}^3 \nu_k \mathcal{S}_1^{(k)}(s), \quad \tilde{N}_1(s) = \sum_{k=0}^1 \tilde{\nu}_k \tilde{\mathcal{S}}_1^{(k)}(s), \quad (34)$$

where $\mathcal{S}_1^{(k)}, \tilde{\mathcal{S}}_1^{(k)}$ are independent solutions. In the case of \widetilde{M}_1 , a single parameter is involved and one has

$$\widetilde{M}_1(s) = \tilde{\mu}_1 \tilde{\mathcal{S}}_1(s), \quad \widehat{\widetilde{M}}_1(s) = \frac{\tilde{\mu}_1}{2\kappa(s)} \int_{-1}^{+1} dz (-9(s-s_0)z - 3\kappa(s)z^2) \tilde{\mathcal{S}}_1(t(z)) \quad (35)$$

with $s_0 = m_K^2 + m_\pi^2/3$. The 10 coefficients $\mu_k, \nu_k, \tilde{\nu}_k$ have been determined in ref. [23] using experimental data on the Dalitz plot behaviour of the $K \rightarrow 3\pi$ decays. The 11th coefficient, $\tilde{\mu}_1$, appears, as already mentioned, only in the $K_S \rightarrow \pi^+\pi^-\pi^0$ amplitude and could not be

determined from the decay data. The reason for this can be clearly seen from eq. (32): the part involving the function \widetilde{M}_1 (first line in this equation) is antisymmetric with respect to the three permutations $t \leftrightarrow u$, $u \leftrightarrow s$, $s \leftrightarrow t$ and thus vanishes along the three lines $t = u$, $u = s$, $s = t$ which meet at the centre of the Dalitz plot. This part of the $K_S \rightarrow \pi^+\pi^-\pi^0$ amplitude, even though enhanced in principle by the $\Delta I = 1/2$ rule, is thus strongly suppressed with respect to the $\Delta I = 3/2$ part, which is antisymmetric under $t \leftrightarrow u$ exchange only, in the whole physical decay region. Here, however, the $K_S \rightarrow \pi^+\pi^-\pi^0$ amplitude will be used away from the physical decay region. In this situation the $\Delta I = 1/2$ part of the amplitude is no longer suppressed, it should be comparable to or even larger than the $\Delta I = 3/2$ amplitude. This feature will allow us to obtain a determination of the parameter $\tilde{\mu}_1$.

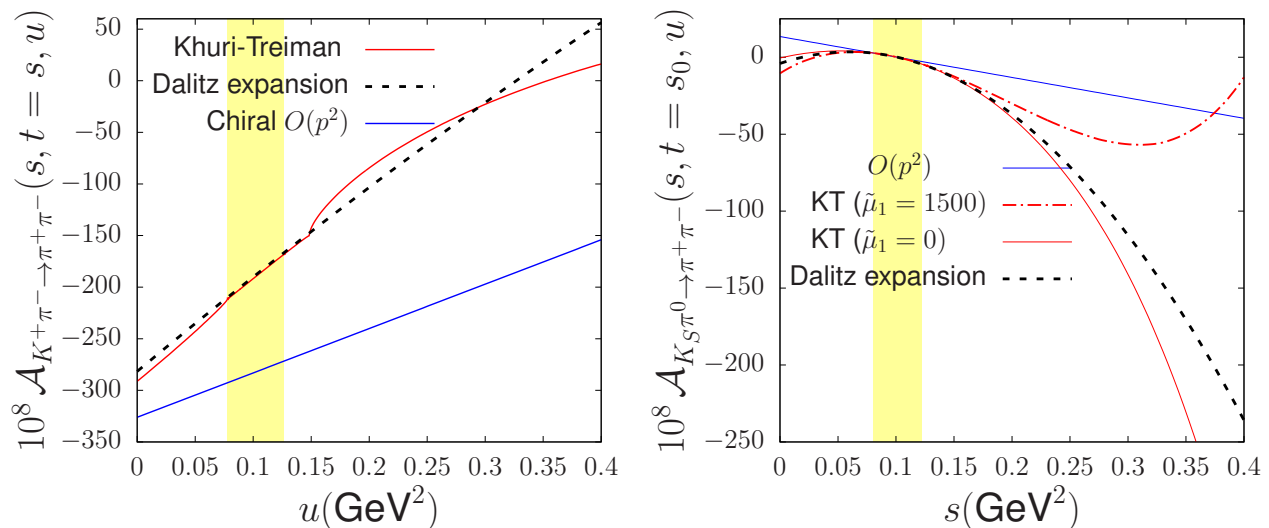


Figure 7: Comparison of the real parts of the Khuri-Treiman amplitudes with their Dalitz-plot expansions at quadratic order. The yellow band indicates the physical region. The left figure shows the $K^+\pi^- \rightarrow \pi^+\pi^-$ amplitude along the line $s = t$ as a function of the variable u . The figure on the right shows the $K_S\pi^0 \rightarrow \pi^+\pi^-$ amplitude fixing $t = s_0$ as a function of the variable s . The figures also show the chiral expansions of both amplitudes at order p^2 , taking $G_8 = G_F/\sqrt{2}V_{ud}V_{us} \times 3.62$ and $G_{27} = G_F/\sqrt{2}V_{ud}V_{us} \times 0.29$ from the review [58].

5 Results

5.1 $K \rightarrow 3\pi$: Dispersive amplitudes versus their X, Y expansion

Because of the importance of the $K \rightarrow 3\pi$ amplitudes in the construction of the $W_{+,s}$ form factors let us start with a brief comparison between the amplitudes derived from the Khuri-Treiman formalism and their expansions to quadratic order as a function of the Dalitz variables

X, Y as used in the B1L description [17]. This is illustrated in fig. 7. The figure also shows the $K \rightarrow 3\pi$ amplitudes computed at chiral order p^2 (entering in the evaluation of $W_{+,S}$ at chiral order p^4). We recall their expressions below (e.g. [59])

$$\begin{aligned}\mathcal{A}_{K^+\pi^-\rightarrow\pi^+\pi^-}(s, t, u)|_{p^2} &= G_8(u - m_K^2 - m_\pi^2) + G_{27}\left(-\frac{13}{3}u + m_K^2 + \frac{13}{3}m_\pi^2\right) \\ \mathcal{A}_{K_S\pi^0\rightarrow\pi^+\pi^-}(s, t, u)|_{p^2} &= G_{27}(t - u)\frac{-15m_K^2 + 10m_\pi^2}{6(m_K^2 - m_\pi^2)}.\end{aligned}\quad (36)$$

We first remark that the signs of the real parts of the $K \rightarrow 3\pi$ KT amplitudes are in agreement with those used in the B1L model [17] and they also agree with the chiral $O(p^2)$ amplitudes provided the two chiral couplings G_8 and G_{27} are taken to be positive. These signs will enable us to define the signs and the phases of the W_+ , W_S amplitudes. Figure 7 also shows that the Dalitz expansion provides a precise description⁴ inside the physical decay regions (yellow bands in the figures) that remains qualitatively acceptable in a rather large region. Figure 7 (right) shows the effect of the parameter $\tilde{\mu}_1$ which induces a cubic term in the Dalitz expansion. This term becomes important away from the physical decay region.

5.2 Determination of $\tilde{\mu}_1$

We have argued that the combination $W^{[3/2]}(s) = W_+(s) + W_S(s)$ that corresponds to a $K\pi$ isospin $I = 3/2$ should satisfy a dispersive representation with no subtraction parameter. We also assumed that the $\Delta I = 1/2$ rule leads to a suppression of the contributions from the $I = 0$ resonances relative to those of the $I = 1$ resonances in this combination. Then, for small values of s , one should be able to compute $W_+(s) + W_S(s)$ reliably by including the dominant contribution from the $\rho(770)$ resonance. In the dispersive approach, this contribution is included in the $\pi\pi$ discontinuity through both the pion form factor $F_V^{\pi\pi}$ and the $K\pi \rightarrow \pi\pi$ amplitudes. These amplitudes are known up to a linear dependence on the parameter $\tilde{\mu}_1$ appearing in the $K_S \rightarrow \pi^+\pi^-\pi^0$ amplitude, see eqs. (33) and (35). Fig. 8 illustrates the influence of this parameter on the discontinuity function $\text{disc}[W_S]_{\pi\pi}$. One sees that the dependence is small at low energies $\sqrt{s} \lesssim 0.5$ GeV, as expected, but significant in the region of the resonance peak. Computing the dispersive integral for $W^{[3/2]}$ from eq. (21) at $s = 0$ leads to the following linear relation between the parameter $\tilde{\mu}_1$ and $a_+ + a_S$

$$\begin{aligned}10^8 G_F m_K^2 (a_+ + a_S) &= -952.4 \pm 30.7 + i(2.17 \pm 0.82) \\ &+ 10^8 \tilde{\mu}_1 (0.73 \pm 0.04 + i(1.12 \pm 1.39) \cdot 10^{-3}),\end{aligned}\quad (37)$$

where the central value corresponds to a cutoff $\Lambda = 1.2$ GeV and the errors are generated by varying the Khuri-Treiman parameters and increasing the value of the integration cutoff up to 1.8 GeV.

⁴We used the expansion coefficients as given in Table 5 of ref.[23]. Let us note that the real part of the parameter ξ'_3 was given with the wrong sign in this table.

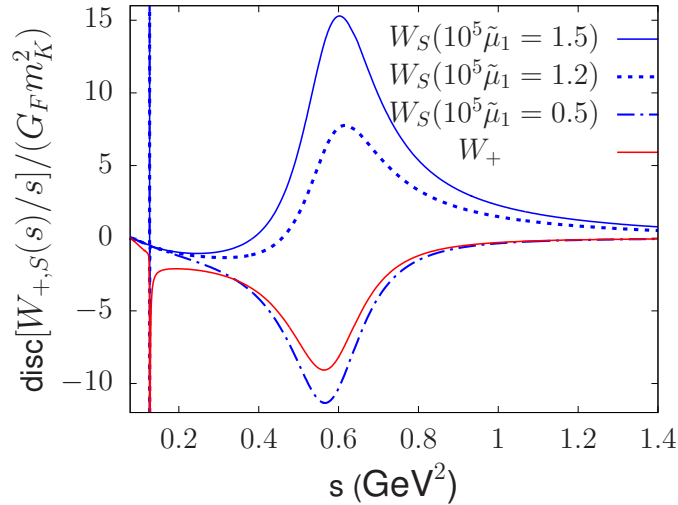


Figure 8: Illustration of the behaviour of the $\pi\pi$ discontinuities $\text{disc}[W_+]_{\pi\pi}$ and $\text{disc}[W_S]_{\pi\pi}$ as a function of s . Notice the singularity at $s = (m_K - m_\pi)^2$ (see sec. 2.3). The function $\text{disc}[W_S]_{\pi\pi}$ is shown for several values of the parameter $\tilde{\mu}_1$.

Making use of the relation (37), the pair of dispersive representations (21), (25) provide a determination of W_+ and W_S in terms of the two parameters a_+ , a_S . The value of a_+ has been determined by a number of experiments by measuring the energy distribution in $K^\pm \rightarrow \pi^\pm e^+ e^-$ or $K^\pm \rightarrow \pi^\pm \mu^+ \mu^-$ and extrapolating to $s = 0$ using the B1L model or simpler descriptions (see ref. [21] for a detailed discussion and a list of references). Let us quote here the recent results by the NA62 collaboration [6]:

$$\begin{aligned} a_+ &= -(0.575 \pm 0.012), & \chi^2/\text{ndf} &= 45.1/48 \\ a_+ &= +(0.373 \pm 0.012), & \chi^2/\text{ndf} &= 56.4/48 \end{aligned} \quad (38)$$

based on the $K^+ \rightarrow \pi^+ \mu^+ \mu^-$ channel. Estimates of a_S have been derived from the measurements of the $K_S \rightarrow \pi^0 \ell^+ \ell^-$ branching fractions using the B1L model additionally assuming a VMD-type relation between b_S and a_S . From the $e^+ e^-$ channel, ref. [9] gives $a_S = \pm(1.06_{-0.21}^{+0.26} \pm 0.07)$ while in ref. [13] the value $a_S = \pm(1.08_{-0.21}^{+0.26})$ is found. From the $\mu^+ \mu^-$ channel, ref. [10] obtains $a_S = \pm(1.54_{-0.32}^{+0.40} \pm 0.06)$. A value of $|a_S|$ lying in the range [1, 1.5] has also been obtained in refs. [14, 15]. The sum $a_+ + a_S$ should therefore satisfy

$$-2 \lesssim a_+ + a_S|_{\text{exp}} \lesssim +2. \quad (39)$$

Using eq. (37) we deduce that $\tilde{\mu}_1$ must be positive and lie in the range

$$519 \lesssim 10^8 \tilde{\mu}_1 \lesssim 2089. \quad (40)$$

The order of magnitude of $\tilde{\mu}_1$ is reasonable if we compare it with the parameter μ_3 which plays an analogous role in the description of the $\Delta I = 1/2$ function M_1 and was determined to be

$10^8 \mu_3 = -1072.6 \pm 13.6$ in ref. [23]. The analogous parameters that appeared in the $\Delta I = 3/2$ functions N_1, \tilde{N}_1 were somewhat smaller $10^8 \nu_3 = 123.9 \pm 12.6$ and $10^8 \tilde{\nu}_1 = 433.2 \pm 12.2$ in agreement with the expectation from the $\Delta I = 1/2$ enhancement rule. This rule would lead to favour the upper half of the range (40) and, then, to the expectation that $a_+ + a_S$ should be positive.

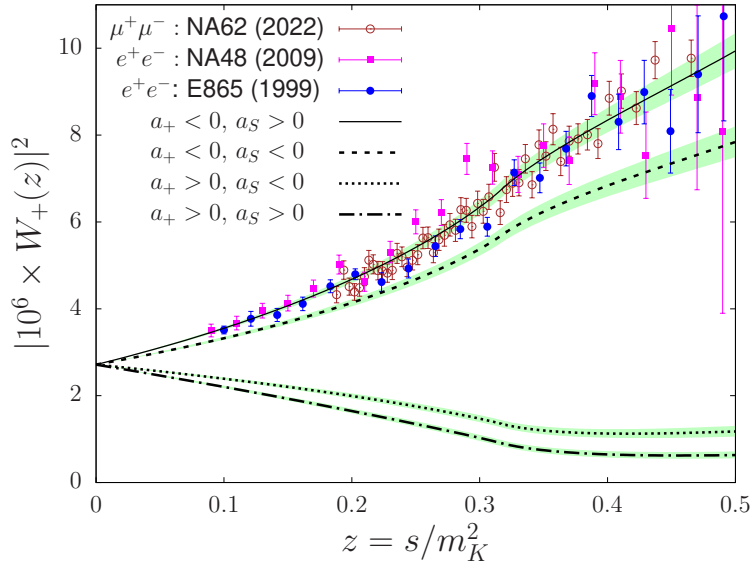


Figure 9: Results for $|W_+|^2$ corresponding to different choices of signs for $a_{+,S}$: $a_+ = \mp 0.575$, $a_S = \pm 1.06$, compared to the experimental data from refs. [3, 4, 6]

5.3 Results for $W_+(s)$

Let us now present the results for the amplitude W_+ . Being deduced from a coupled system of equations it is expected to depend on both a_+ and a_S . For illustration, we choose $a_+ = \mp 0.575$ (the negative value corresponding to the central result from the NA62 experiment [6]) and $a_S = \pm 1.06$ (from ref. [9]). The results for $|W_+(s)|^2$ corresponding to the four combinations of a_+, a_S sign values are shown in fig. 9 and compared with the experimental determinations from refs. [3, 4, 6]. The figure shows that a positive value for a_+ can be ruled out since, in this case, $|W_+|^2$ is a decreasing function of s (see also below), which is in disagreement with the experimental results. The figure also shows that W_+ has a clear sensitivity to the value of a_S . The best agreement with the experimental data is achieved when a_S is positive. The error bands which are shown in the figure are generated by varying the Khuri-Treiman parameters as well as the integration cutoff parameter Λ . An additional uncertainty, however, is associated with the contributions of the $I = 0$ resonances $\omega(782), \phi(1020)$ which we will discuss below. The pair of values $a_+ = -0.575, a_S = +1.06$ leads to an amplitude $|W_+|$ which agrees reasonably

well with experiment. Computing the corresponding branching fractions we find

$$\begin{aligned} BF[K^+ \rightarrow \pi^+ e^+ e^-] &= (3.01 \pm 0.05) \cdot 10^{-7} \\ BF[K^+ \rightarrow \pi^+ \mu^+ \mu^-] &= (8.89 \pm 0.24) \cdot 10^{-8} \end{aligned} \quad (41)$$

which are consistent with the experimental values (from the PDG [60])

$$\begin{aligned} BF[K^+ \rightarrow \pi^+ e^+ e^-]_{exp} &= (3.00 \pm 0.09) \cdot 10^{-7} \\ BF[K^+ \rightarrow \pi^+ \mu^+ \mu^-]_{exp} &= (9.17 \pm 0.14) \cdot 10^{-8} \end{aligned} \quad (42)$$

For small values of s a linear approximation of the real part of $W_+(s)$ holds $W_+(s) \simeq G_F[a_+ m_K^2 + \bar{b}_+ s]$ in which the slope parameter \bar{b}_+ can be shown from the dispersive representations to be a linear function of a_+ and a_S of the following form

$$\bar{b}_+ = -0.551 + 0.214 a_+ - 0.100 a_S . \quad (43)$$

This formula shows that the slope of the function $W_+(s)$ at the origin is always negative provided a_+ , a_S have the usual order of magnitude. This explains why the modulus of $W_+(s)$ is a decreasing function of s when a_+ is positive, see fig. 9.

Finally, it is interesting to compare the amplitude W_+ computed from the pair of dispersive representations (21) (25) to the one evaluated with the B1L expression (1) using the central values of the parameters determined by the NA62 experiment⁵: $a_+ = -0.575$, $b_+ = -0.722$. This is shown in fig 10. The real parts are seen to be nearly identical below the $\pi\pi$ threshold and slightly different above. The imaginary parts differ somewhat more significantly: the dispersive part being larger in magnitude than the B1L one by approximately a factor of two in the upper part of the physical energy range. One also notices that the imaginary part in the dispersive amplitude does not vanish below the $\pi\pi$ threshold. This reflects a contribution to the imaginary part associated with $K \rightarrow 3\pi$ followed by $3\pi \rightarrow \gamma^* \pi$. In the chiral expansion this contribution appears at two-loops.

5.4 Results for $W_S(s)$

We turn now to the amplitude W_S . Experimentally, two branching fraction measurements are available, performed by the NA48 collaboration: a) of the mode $K_S \rightarrow \pi^0 e^+ e^-$ in the energy range $E_{ee} > 165$ MeV [9] and b) of the mode $K_S \rightarrow \pi^0 \mu^+ \mu^-$ (ref. [10]). We reproduce these two results below

$$\begin{aligned} BF(K_S \rightarrow \pi^0 e^+ e^-)|_{E_{ee} > 165 \text{ MeV}} &= (3.0_{-1.2}^{+1.5} \pm 0.2) \cdot 10^{-9} \\ BF(K_S \rightarrow \pi^0 \mu^+ \mu^-) &= (2.9_{-1.2}^{+1.5} \pm 0.2) \cdot 10^{-9} \end{aligned} \quad (44)$$

and compare them with the branching fractions computed in the dispersive approach varying the value of a_S (with a_+ fixed) in fig. 11. One sees from the figure that there are two values of

⁵We note that the parameter b_+ in the B1L model is numerically very close to the parameter \bar{b}_+ corresponding to the derivative of W_+ at $s=0$, $\bar{b}_+ = b_+ - 0.092$.

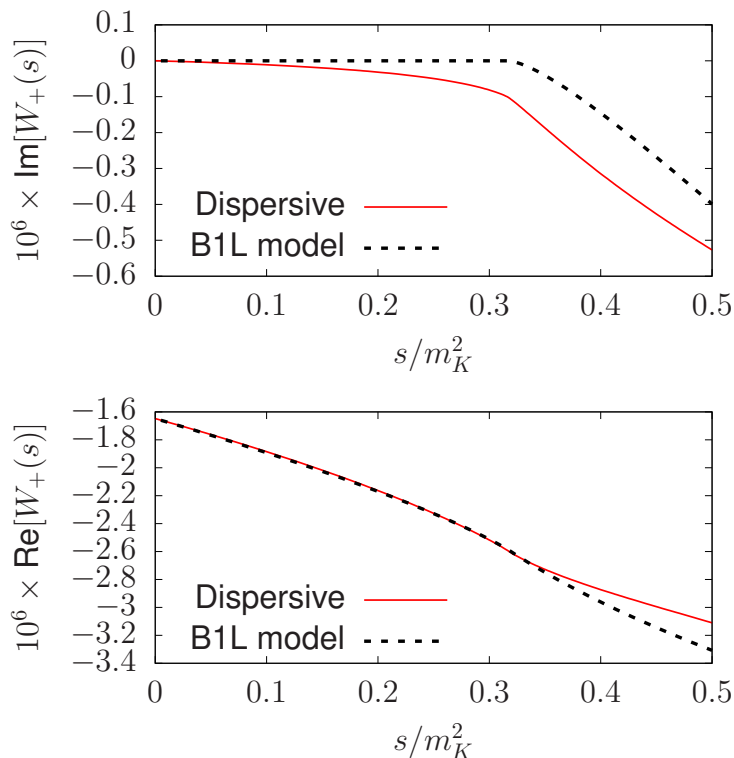


Figure 10: Comparison of the real (lower plot) and imaginary parts (upper plot) of the W_+ amplitude computed from the dispersive representation with $a_+ = -0.575$, $a_S = 1.06$ (red lines) and from the B1L one with the same a_+ and $b_+ = -0.722$ (black dashed lines).

a_S for which agreement with the experimental branching ratios can be achieved. Computing the χ^2 one finds that the two minimums have approximately the same χ^2 value, $\chi^2 \simeq 1.27$ and they correspond to the following results for a_S ,

$$a_S = -1.15 \pm 0.20, \quad a_S = +1.10 \pm 0.20 \quad (45)$$

which are in agreement with those estimated earlier [9, 10, 13, 14]. Computing the $\ell^+\ell^-$ branching fractions from the dispersive amplitudes with either one of the two values of a_S given in (45) gives approximately the same result

$$\begin{aligned} BF(K_S \rightarrow \pi^0 e^+ e^-)|_{E_{ee} > 165 \text{ MeV}} &= (3.83 \pm 1.34) \cdot 10^{-9} \\ BF(K_S \rightarrow \pi^0 \mu^+ \mu^-) &= (1.71 \pm 0.60) \cdot 10^{-9} . \end{aligned} \quad (46)$$

The curves in fig. 11 are nearly symmetric with respect to $a_S = 0$. Therefore, measuring the branching fractions with a higher precision would provide a strong test of the approach but will not allow to determine the sign of a_S .

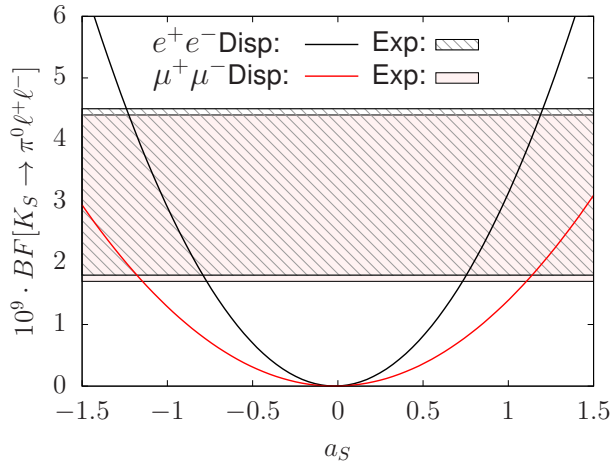


Figure 11: Branching fractions for $K_S \rightarrow \pi^0 e^+ e^-$ ($m_{ee} > 0.165$ GeV) and $K_S \rightarrow \pi^0 \mu^+ \mu^-$ as a function of a_S (with $a_+ = -0.575$ fixed) in the dispersive approach compared with the experimental results [9, 10].

Some sensitivity to the sign of a_S is exhibited in the energy dependence of $|W_S(s)|^2$. The dispersive results for this quantity, taking $a_S \pm 1.06$ and $a_+ = -0.575$ are shown in fig. 12. Clearly, the difference between the results corresponding to the two signs is not as marked as it was in the case of W_+ and a_+ . However, if experimental results were available for a few energy bins, a one-parameter fit could be able to determine the sign of a_S .

For small values of the energy s , as before, the following linear approximation of W_S holds: $W_S(s) \simeq G_F[a_S m_K^2 + \bar{b}_S s]$ and the slope parameter \bar{b}_S is a linear function of a_+ and a_S

$$\bar{b}_S = 0.259 + 0.186 a_+ + 0.500 a_S. \quad (47)$$

This formula shows that, assuming that $a_+ \simeq -0.575$ and $|a_S| \gtrsim 1$, the sign of the slope at the origin is the same as the sign of a_S . The presence of the term which is not proportional to a_S in eq. (47) allows, in principle, to distinguish between the two sign possibilities based on the amplitude squared.

5.5 Additional contributions: ω and ϕ resonances

An approximate evaluation of the contributions from the $I = 0$ resonances $\omega(782)$, $\phi(1020)$ to the form factors $W_{+,S}$ can be performed assuming nonet symmetry and $\Delta I = 1/2$ dominance. For this purpose, we start from the resonance-chiral Lagrangian proposed in ref. [61] which generalises to the $\Delta S = 1$ sector (and $\Delta I = 1/2$) the formalism first introduced in ref. [62] for the strong, electromagnetic and semi-leptonic sectors. In this formalism, vector and axial-vector resonances are described with antisymmetric tensor fields. These can be ascribed a chiral order p^2 and the Lagrangian written in ref. [61] (we refer to this article for details on the notation

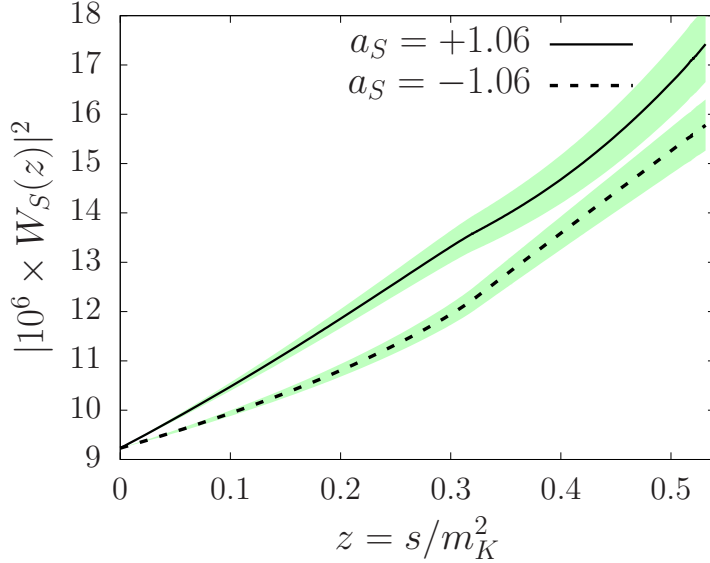


Figure 12: Predicted dependence of $|W_S|^2$ as a function of s for two different signs of a_S .

used below) contains a complete set of independent terms which have a chiral order p^4 . At this order, flavour symmetry is left unbroken, such that the vector resonances are degenerate in mass if we further assume nonet symmetry i.e. that double-trace terms are suppressed by the OZI rule. There are three relevant terms involving vector mesons which contribute to the $W_{+,S}$ form factors⁶,

$$\mathcal{L}_{\Delta S=1}(V) = g_V^1 \langle \Delta \{V_{\mu\nu}, f_+^{\mu\nu}\} \rangle + ig_V^5 \langle \Delta \{V_{\mu\nu}, [u^\mu, u^\nu]\} \rangle + ig_V^6 \langle \Delta u_\mu V^{\mu\nu} u_\nu \rangle, \quad (48)$$

where $\Delta = u\lambda_6 u^\dagger$ and we have also assumed that the OZI suppressed term $\langle V^{\mu\nu} \rangle \langle \Delta [u_\mu, u_\nu] \rangle$ can be neglected. The following terms from the ordinary sector are also involved,

$$\begin{aligned} \mathcal{L}(V) = & -\frac{1}{2} \langle \nabla^\lambda V_{\lambda\mu} \nabla_\nu V^{\nu\mu} - \frac{1}{2} M_V^2 V_{\mu\nu} V^{\mu\nu} \rangle \\ & + \frac{F_V}{2\sqrt{2}} \langle V_{\mu\nu} f_+^{\mu\nu} \rangle + \frac{iG_V}{\sqrt{2}} \langle V_{\mu\nu} u^\mu u^\nu \rangle \end{aligned} \quad (49)$$

as well as terms from the $O(p^2)$ chiral Lagrangian

$$\mathcal{L}^{(2)} = \frac{F_\pi^2}{4} \langle u^\mu u_\mu + \chi^+ \rangle, \quad \mathcal{L}_{\Delta S=1}^{(2)} = G_8 F_\pi^4 \langle \Delta u^\mu u_\mu \rangle. \quad (50)$$

We can now compute the radiative amplitudes $K \rightarrow \pi\gamma^*$ from the Lagrangian terms given above at tree level. The resulting amplitudes are expressed as a sum of poles. The $I = 3/2$

⁶Unlike in the vector field formalism (e.g. [63, 64]) axial-vector resonances do not contribute to the $W_{+,S}$ form factors in the antisymmetric tensor field formalism at this chiral order.

a_S	$10^8 g_V^1/F_\pi$	$10^8 g_V^5/F_\pi$	$10^8 g_V^6/F_\pi$
+1.06	-3.38	-0.06	-5.91
-1.06	0.15	2.24	-1.42

Table 1: Approximate values of the three coupling constants g_V^1, g_V^5, g_V^6 corresponding to two input values of a_S .

combination has no contributions from the $I = 0$ resonances, it reads,

$$\frac{W_{res}^{[3/2]}(s)}{16\pi^2 m_K^2} = -\frac{\sqrt{2}F_V (g_V^6 + \sqrt{2}G_8 G_V F_\pi^2)}{F_\pi^2 (M_\rho^2 - s)}, \quad (51)$$

and the $I = 1/2$ combination has the following expression

$$\begin{aligned} \frac{W_{res}^{[1/2]}(s)}{16\pi^2 m_K^2} = & \frac{4\sqrt{2}G_V}{F_\pi^2} \frac{g_V^1}{M_{K^*}^2 - s} + \frac{F_V}{\sqrt{2}F_\pi^2} \left[\frac{6g_V^5 - g_V^6}{M_\rho^2 - s} - \frac{2g_V^5 + g_V^6}{M_\omega^2 - s} + \frac{4g_V^5}{M_\phi^2 - s} \right] \\ & + \frac{G_8 G_V F_V}{m_K^2 - m_\pi^2} \left[\frac{-4m_K^2 + m_\pi^2}{M_\rho^2 - s} + \frac{m_\pi^2}{M_\omega^2 - s} + \frac{2m_\pi^2}{M_\phi^2 - s} \right]. \end{aligned} \quad (52)$$

The $\rho(770)$ resonance corresponds to a pole on the second Riemann sheet in the dispersive amplitudes. Equating the residues of this pole in the W_+ , W_S amplitudes with those in the resonance model allows to determine the values of the two couplings g_V^5 , g_V^6 . Similarly the coupling g_V^1 can be estimated from the residue of the $K^*(892)$ pole. In practice, we have estimated these couplings more simply by fitting the imaginary parts of the amplitudes in the resonance model, after including physical values for the masses and the widths in the denominators, to the imaginary parts of the dispersive amplitudes. The resulting values of the couplings g_V^i are collected⁷ in table 1.

The radiative amplitudes being approximately linear in s in the physical decay region $[4m_l^2, (m_K - m_\pi)^2]$, we can characterise in a simple way the effect of the $I = 0$ resonances ω, ϕ from their contributions to the derivative at $s = 0$, i.e. to the slope parameter. Computing the derivative from eq. (52) one obtains, in the nonet symmetry limit,

$$G_F \bar{b}_{\omega, \phi}^{[1/2]} = \frac{16\pi^2 m_K^2 F_V}{\sqrt{2}F_\pi^2 M_V^4} \left[2g_V^5 - g_V^6 + \frac{3\sqrt{2}G_8 G_V F_\pi^2 m_\pi^2}{m_K^2 - m_\pi^2} \right]. \quad (53)$$

The corresponding slopes of $W_{+,S}$ are simply related to $\bar{b}_{\omega, \phi}^{[1/2]}$ by: $\bar{b}_+|_{\omega, \phi} = \bar{b}_{\omega, \phi}^{[1/2]}/3$, $\bar{b}_S|_{\omega, \phi} = -\bar{b}_{\omega, \phi}^{[1/2]}/3$. One sees from the numbers given in table 1 that the slopes generated by ω, ϕ are rather small and nearly independent of the sign of a_S :

$$\bar{b}_+|_{\omega, \phi} \simeq +0.25 (a_S > 0), \quad \bar{b}_+|_{\omega, \phi} \simeq +0.26 (a_S < 0) \quad (54)$$

⁷The following numerical input values are used: $G_V = 53.0$, $F_V = 154.0$, $F_\pi = 92.2$ (all in MeV) and $G_8 = 6.54 \cdot 10^{-6} \text{ GeV}^{-2}$.

using $M_V = M_\omega$. This reflects the fact that $\text{Im}[W_+]$ (unlike $\text{Re}[W_+]$), from which the combination $2g_V^5 - g_V^6$ is derived, has a very small dependence on a_S at low energy and up to the ρ mass.

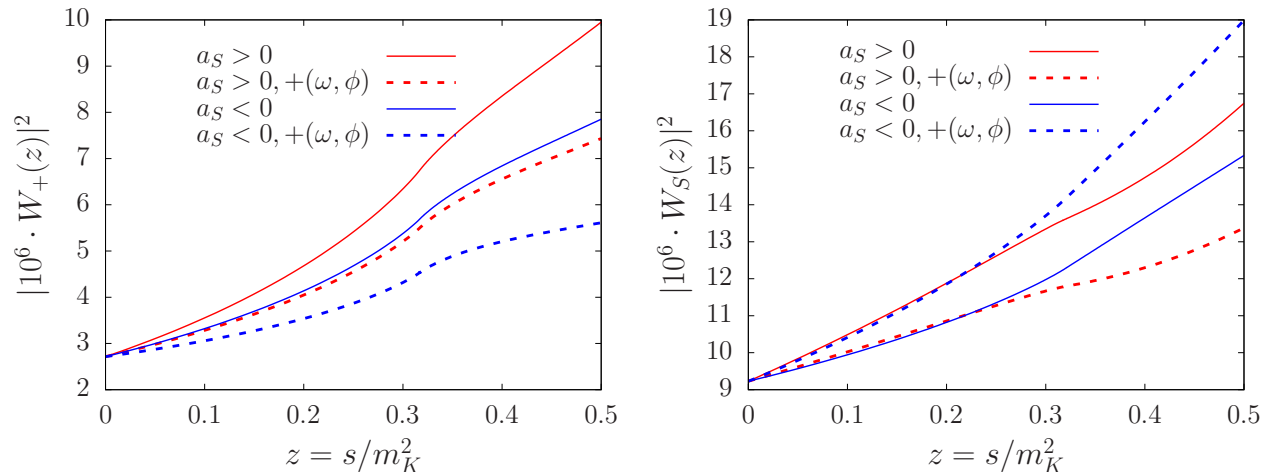


Figure 13: Contributions of the $I = 0$ resonances ω , ϕ to W_+ (left) and W_S (right). The values at $s = 0$ are fixed with $a_+ = -0.575$ and $a_S = \pm 1.06$. The solid and dashed red lines show the dispersive results when $a_S > 0$ without (solid) and with (dashed) the $I = 0$ resonances. The solid and dashed blue lines show the results without and with the $I = 0$ resonances when a_S is negative.

The results of including the effects of the $I = 0$ resonances, estimated in the way described above, is illustrated in fig. 13. In the case of W_+ , they decrease the modulus squared of the amplitudes in both cases of $a_S > 0$ and $a_S < 0$. The former case thus remains favoured by comparison with the experimental data. A similar effect of the $I = 0$ resonances to W_+ was observed also in the factorisation approach [29, 65]. In the case of $|W_S|^2$, the $I = 0$ resonances modify significantly the difference between the results corresponding to $a_S > 0$ and $a_S < 0$ (see fig. 13, right).

5.6 Additional contributions: higher mass resonances

We can make a simple qualitative estimate of the role of higher mass resonances in the following way. In the dispersive representation (24) the contributions from the energy region above the cutoff Λ are absorbed into a constant $C^{[1/2]}(\nu)$. As shown in [21] the dependence on the scale ν of this constant can be generated in a Regge-type model involving a sum over an infinite set of resonances with equally spaced masses squared such that the asymptotic behaviour in s is of the form $\sim \log(s/\nu^2)$. The coefficient of this logarithmic function must coincide with the leading term in the short-distance operator-product expansion of $T(j_\mu(x) \sum C_i O_i(y))$. Using the model developed in [21], and keeping the resonances which have a mass higher than 1 GeV in the sum amounts to replace $C^{[1/2]}(\nu)$ by a constant independent of ν plus a function $C^{[1/2]}(s; \nu)$ of the

following form

$$C^{[1/2]}(s; \nu) = \frac{G_F}{\sqrt{2}} V_{ud} V_{us} \frac{8m_K^2}{3} (N_c(C_1 - C_4) + C_2 - C_3) \left(\frac{5}{3} + \log \frac{\nu^2}{M^2} - \psi\left(3 - \frac{s}{M^2}\right) \right). \quad (55)$$

The resonance poles generated by the ψ function correspond to masses $M_n = M\sqrt{n+2}$ with $n \geq 1$. Taking $M = 0.87$ GeV as obtained in [15] gives $M_n = 1.51, 1.74, 1.95, \dots$ GeV. Finally, the contribution from the infinite sum over these higher mass states to the derivative at $s = 0$ is easily obtained from (55),

$$G_F \bar{b}_{M_n > \Lambda}^{[1/2]} = \frac{G_F}{\sqrt{2}} V_{ud} V_{us} \frac{8m_K^2}{3M^2} (N_c(C_1 - C_4) + C_2 - C_3) \psi'(3) \simeq -2.82 \cdot 10^{-3} \quad (56)$$

using $C_1 = -0.506$, $C_2 = 1.270$, $C_3 = 0.013$, $C_4 = -0.034$ (values at a scale $\nu = 1$ GeV, in the NDR scheme, taken from [66]) and $\psi'(3) = \pi^2/6 - 5/4$. The contribution to the slope parameter from these higher mass states, in this model, is seen to be essentially negligible being smaller than the corresponding slope generated by the light resonances ω, ϕ by two orders of magnitude.

6 Conclusions

We have developed a description of the $K \rightarrow \pi \ell^+ \ell^-$ amplitudes W_+ and W_S in a dispersive theoretical approach which goes beyond previous studies (e.g. [17]) in taking explicitly into account, in particular, the effects of the light vector resonances $\rho(770)$, $K^*(892)$. This is achieved, on the one hand, by making use of new results on the $K \rightarrow 3\pi$ amplitudes [23], which have a domain of validity extending beyond the physical decay region and, on the other hand, by including the $K\pi$ states into the unitarity relations and the corresponding integral representations. The structure of these is compatible with the requirement that the QCD scale dependence should cancel upon adding the contribution associated with the operator O_{7V} .

Considering the two combinations $W^{[1/2]} \equiv 2W_+ - W_S$ and $W^{[3/2]} = W_+ + W_S$ we have investigated dispersive representations which involve the minimal number of subtraction constants compatible with their asymptotic behaviours. The resulting coupled system of equations for W_+ , W_S are given in eqs. (21) and (25) depends on only two parameters a_+ and a_S .

Other light vector resonances are present, in particular $\omega(782)$, $\phi(1019)$, but their influence on the $W_{+,S}$ amplitudes cannot be accounted for in the same way as was done for the ρ and the K^* resonances, because the corresponding discontinuities involve amplitudes, $K\pi \rightarrow 3\pi$, $K\bar{K} \rightarrow K\pi$ which cannot be accessed experimentally. We estimated their contributions in an approximate way by appealing to nonet symmetry, $\Delta I = 1/2$ dominance, and relying on a chiral-resonance Lagrangian, finding them to be less important than the $I = 1, 1/2$ resonances but possibly significant. In a general way, the isoscalar resonances can be accounted for model independently by introducing one additional subtraction parameter in the $W^{[1/2]}$ dispersive representation.

The main outcomes of our dispersive representations are illustrated in figs. 9 and 12 showing the results for the amplitudes squared $|W_+|^2$ and $|W_S|^2$ corresponding to different signs of a_+ and a_S . A positive sign for a_+ is seen to be clearly excluded in this approach. Of more interest, perhaps, is the sign of a_S . Fig. 12 shows that the s dependence of $|W_S|^2$ has a certain sensitivity to this sign but it appears to be weakened upon including the effects of the $I = 0$ resonances (see fig. 13). However, $|W_+|^2$ is also sensitive to the sign of a_S , because of the coupling between W_+ and W_S , as one can see rather clearly in fig. 9. Given some improved data on $|W_S|^2$ one could hope to derive strong constraints both on $|a_S|$ and its sign by performing a combined fit of the $|W_+|^2$ and $|W_S|^2$ data. At the moment, we note that the curve which corresponds to the central values $a_+ = -0.575$, $a_S = +1.06$ (taken simply from the literature) is in rather good agreement with the experimental data.

Another aspect of our analysis concerns the $\Delta I = 1/2$ part of the $K_S \rightarrow \pi^+\pi^-\pi^0$ amplitude, which has not been determined so far. In the KT approach this part involves a single parameter $\tilde{\mu}_1$ and we have derived a linear relation between $\tilde{\mu}_1$ and the sum $a_+ + a_S$ (eq. (37)) which allows to determine $\tilde{\mu}_1$. The effect of this $\Delta I = 1/2$ amplitude is chirally suppressed inside the Dalitz plot but it is not excluded that it could be measured in the future.

References

- [1] J.H. Christenson, J.W. Cronin, V.L. Fitch, R. Turlay, Phys. Rev. Lett. **13**, 138 (1964)
- [2] G. Anzivino et al., Eur. Phys. J. C **84**(4), 377 (2024), 2311.02923
- [3] R. Appel et al. (E865), Phys. Rev. Lett. **83**, 4482 (1999), hep-ex/9907045
- [4] J.R. Batley et al. (NA48/2), Phys. Lett. **B677**, 246 (2009), 0903.3130
- [5] J.R. Batley et al. (NA48/2), Phys. Lett. **B697**, 107 (2011), 1011.4817
- [6] E. Cortina Gil et al. (NA62), JHEP **11**, 011 (2022), [Addendum: JHEP 06, 040 (2023)], 2209.05076
- [7] A. Crivellin, G. D’Ambrosio, M. Hoferichter, L.C. Tunstall, Phys. Rev. D **93**(7), 074038 (2016), 1601.00970
- [8] G. D’Ambrosio, A.M. Iyer, F. Mahmoudi, S. Neshatpour, JHEP **09**, 148 (2022), 2206.14748
- [9] J.R. Batley et al. (NA48/1), Phys. Lett. B **576**, 43 (2003), hep-ex/0309075
- [10] J.R. Batley et al. (NA48/1), Phys. Lett. B **599**, 197 (2004), hep-ex/0409011

- [11] H. Nanjo, T. Nomura, F. Dettori et al. (KOTO, LHCb, NA62/KLEVER, US Kaon Interest Group), *Searches for new physics with high-intensity kaon beams*, in *Snowmass 2021 (2022)*, 2204.13394
- [12] A.A. Alves Junior et al., *JHEP* **05**, 048 (2019), 1808.03477
- [13] G. Buchalla, G. D’Ambrosio, G. Isidori, *Nucl. Phys. B* **672**, 387 (2003), hep-ph/0308008
- [14] S. Friot, D. Greynat, E. De Rafael, *Phys. Lett. B* **595**, 301 (2004), hep-ph/0404136
- [15] G. D’Ambrosio, M. Knecht, *Universe* **10**(12), 457 (2024), 2409.08568
- [16] P.A. Boyle, F. Erben, J.M. Flynn, V. Gülpers, R.C. Hill, R. Hodgson, A. Jüttner, F. Ó hÓgáin, A. Portelli, C.T. Sachrajda (RBC, UKQCD), *Phys. Rev. D* **107**(1), L011503 (2023), 2202.08795
- [17] G. D’Ambrosio, G. Ecker, G. Isidori, J. Portolés, *JHEP* **08**, 004 (1998), hep-ph/9808289
- [18] G. Ecker, A. Pich, E. de Rafael, *Nucl. Phys. B* **291**, 692 (1987)
- [19] B. Ananthanarayan, I. Sentitemsu Imsong, *J. Phys. G* **39**, 095002 (2012), 1207.0567
- [20] T.J. Devlin, J.O. Dickey, *Rev. Mod. Phys.* **51**, 237 (1979)
- [21] G. D’Ambrosio, D. Greynat, M. Knecht, *JHEP* **02**, 049 (2019), 1812.00735
- [22] J. Kambor, B.R. Holstein, *Phys. Rev. D* **49**, 2346 (1994), hep-ph/9310324
- [23] V. Bernard, S. Descotes-Genon, M. Knecht, B. Moussallam, *Eur. Phys. J. C* **84**(7), 744 (2024), 2403.17570
- [24] N. Khuri, S. Treiman, *Phys. Rev.* **119**, 1115 (1960)
- [25] R.F. Sawyer, K.C. Wali, *Phys. Rev.* **119**, 1429 (1960)
- [26] N.L. Muskhelishvili, *Singular Integral Equations* (P. Noordhof, Groningen, 1953)
- [27] R. Omnès, *Nuovo Cim.* **8**, 316 (1958)
- [28] M.K. Gaillard, B.W. Lee, *Phys. Rev. D* **10**, 897 (1974)
- [29] L.B. Okun, M.A. Shifman, A.I. Vainshtein, V.I. Zakharov, *Sov. J. Nucl. Phys.* **24**, 427 (1976)
- [30] F.J. Gilman, M.B. Wise, *Phys. Rev. D* **21**, 3150 (1980)
- [31] A.J. Buras, M.E. Lautenbacher, M. Misiak, M. Münz, *Nucl. Phys. B* **423**, 349 (1994), hep-ph/9402347

- [32] G. Isidori, G. Martinelli, P. Turchetti, Phys. Lett. B **633**, 75 (2006), hep-lat/0506026
- [33] R. Karplus, C.M. Sommerfield, E.H. Wichmann, Phys. Rev. **111**, 1187 (1958)
- [34] S. Mutke, M. Hoferichter, B. Kubis, JHEP **07**, 276 (2024), 2406.14608
- [35] J. Kambor, C. Wiesendanger, D. Wyler, Nucl. Phys. B **465**, 215 (1996), hep-ph/9509374
- [36] G. D'Ambrosio, D. Greynat, M. Knecht, Phys. Lett. B **797**, 134891 (2019), 1906.03046
- [37] P. Estabrooks, R.K. Carnegie, A.D. Martin, W.M. Dunwoodie, T.A. Lasinski, D.W.G.S. Leith, Nucl. Phys. B **133**, 490 (1978)
- [38] C. Zemach, Phys. Rev. **133**, B1201 (1964)
- [39] M. Gourdin, Phys.Rept. **11**, 29 (1974)
- [40] H. Leutwyler, *Electromagnetic form-factor of the pion*, in *Continuous advances in QCD. Proceedings, Conference, Minneapolis, USA, May 17-23, 2002* (2002), pp. 23–40, hep-ph/0212324
- [41] T.P. Leplumey, P. Stoffer (2025), 2501.09643
- [42] B. Hyams, C. Jones, P. Weilhammer, W. Blum, H. Dietl et al., Nucl. Phys. B **64**, 134 (1973)
- [43] E. Ruiz Arriola, P. Sanchez-Puertas, Phys. Rev. D **110**(5), 054003 (2024), 2403.07121
- [44] M. Davier, A. Hoecker, A.M. Lutz, B. Malaescu, Z. Zhang, Eur. Phys. J. C **84**(7), 721 (2024), 2312.02053
- [45] J. Lees et al. (BaBar), Phys. Rev. **D86**, 032013 (2012), 1205.2228
- [46] D. Aston et al., Nucl. Phys. B **296**, 493 (1988)
- [47] F. Ambrosino et al. (KLOE), Phys. Lett. B **636**, 166 (2006), hep-ex/0601038
- [48] L. Beldjoudi, T.N. Truong, Phys. Lett. B **351**, 357 (1995), hep-ph/9411423
- [49] B. Moussallam, Eur. Phys. J. C **53**, 401 (2008), 0710.0548
- [50] M. Jamin, A. Pich, J. Portolés, Phys. Lett. B **664**, 78 (2008), 0803.1786
- [51] D.R. Boito, R. Escribano, M. Jamin, JHEP **09**, 031 (2010), 1007.1858
- [52] V. Bernard, JHEP **1406**, 082 (2014), 1311.2569
- [53] R. Barate et al. (ALEPH), Eur. Phys. J. C **11**, 599 (1999), hep-ex/9903015

- [54] D. Epifanov et al. (Belle), Phys. Lett. B **654**, 65 (2007), 0706.2231
- [55] A. Adametz (BaBar), Nucl. Phys. B Proc. Suppl. **218**, 134 (2011)
- [56] M. Jamin, J.A. Oller, A. Pich, Nucl. Phys. B **622**, 279 (2002), hep-ph/0110193
- [57] A. Anisovich, H. Leutwyler, Phys. Lett. B **375**, 335 (1996), hep-ph/9601237
- [58] V. Cirigliano, G. Ecker, H. Neufeld, A. Pich, J. Portolés, Rev. Mod. Phys. **84**, 399 (2012), 1107.6001
- [59] J. Bijnens, P. Dhonte, F. Borg, Nucl. Phys. B **648**, 317 (2003), hep-ph/0205341
- [60] S. Navas et al. (Particle Data Group), Phys. Rev. D **110**(3), 030001 (2024)
- [61] G. Ecker, J. Kambor, D. Wyler, Nucl. Phys. B **394**, 101 (1993)
- [62] G. Ecker, J. Gasser, A. Pich, E. de Rafael, Nucl. Phys. B **321**, 311 (1989)
- [63] G. D'Ambrosio, J. Portolés, Nucl. Phys. B **533**, 494 (1998), hep-ph/9711211
- [64] A.Z. Dubničková, S. Dubnička, E. Goudzovski, V.N. Pervushin, M. Sečanský, Phys. Part. Nucl. Lett. **5**, 76 (2008), hep-ph/0611175
- [65] L. Bergstrom, P. Singer, Phys. Rev. D **43**, 1568 (1991)
- [66] G. Buchalla, A.J. Buras, M.E. Lautenbacher, Rev. Mod. Phys. **68**, 1125 (1996), hep-ph/9512380